

Alma Mater Studiorum Università di Bologna
Archivio istituzionale della ricerca

A novel non-sense and inactivating variant of ST3GAL3 in two infant siblings suffering severe epilepsy and expressing circulating CA19.9

This is the final peer-reviewed author's accepted manuscript (postprint) of the following publication:

Published Version:

Indellicato, R., Domenighini, R., Malagolini, N., Cereda, A., Mamoli, D., Pezzani, L., et al. (2020). A novel non-sense and inactivating variant of ST3GAL3 in two infant siblings suffering severe epilepsy and expressing circulating CA19.9. GLYCOBIOLOGY, 30(2), 95-104 [10.1093/glycob/cwz079].

Availability:

This version is available at: <https://hdl.handle.net/11585/719372> since: 2020-01-31

Published:

DOI: <http://doi.org/10.1093/glycob/cwz079>

Terms of use:

Some rights reserved. The terms and conditions for the reuse of this version of the manuscript are specified in the publishing policy. For all terms of use and more information see the publisher's website.

This item was downloaded from IRIS Università di Bologna (<https://cris.unibo.it/>).
When citing, please refer to the published version.

(Article begins on next page)

A novel non-sense and inactivating variant of ST3GAL3 in two infant siblings suffering severe epilepsy and expressing circulating CA19.9

Rossella Indellicato¹, Ruben Domenighini¹, Nadia Malagolini², Anna Cereda³, Daniela Mamoli⁴, Lidia Pezzani⁵, Maria Iascone⁵, Fabio dall'Olio², Marco Trinchera⁶

¹ Department of Health Sciences, San Paolo Hospital, University of Milan, 20142 Milano, Italy

² Department of Experimental, Diagnostic and Specialty Medicine (DIMES), University of Bologna, 40126 Bologna, Italy

³ Department of Pediatrics, ASST Papa Giovanni XXIII, 24127 Bergamo, Italy

⁴ Neuropsichiatria infantile, ASST Papa Giovanni XXIII, 24127 Bergamo, Italy

⁵ Laboratory of Medical Genetics, ASST Papa Giovanni XXIII, 24127 Bergamo, Italy

⁶ Department of Medicine and Surgery (DMC), University of Insubria, 21100 Varese, Italy

Corresponding author: Marco Trinchera, Dipartimento di Medicina e Chirurgia, Università dell'Insubria, via JH Dunant 5, 21100 Varese, Italy, email: marco.trinchera@uninsubria.it (to whom proofs and reprints should be addressed)

Running Title: Novel ST3GAL3 variant

Key words: Congenital disorders of glycosylation / Ganglioside / Glycosphingolipid / Sialyltransferase

Supplementary Data: Supplementary Table S1, Supplementary Figures S1 and S2, Supplementary Methods.

Abstract

Three missense variants of ST3GAL3 are known to be responsible for a congenital disorder of glycosylation determining a neurodevelopmental disorder (intellectual disability/epileptic encephalopathy). Here we report a novel non-sense variant, p.Y220*, in two di-chorionic infant twins presenting a picture of epileptic encephalopathy with impaired neuromotor development. Upon expression in HEK-293T cells, the variant appears totally devoid of enzymatic activity in vitro, apparently accumulated with respect to the wild type or the missense variants, as detected by western blot, and in large part properly localized in the Golgi apparatus, as assessed by confocal microscopy. Both patients were found to efficiently express the CA19.9 antigen in the serum despite the total loss of ST3GAL3 activity, which thus appears replaceable from other ST3GALs in the synthesis of the sialyl-Lewis a epitope. Kinetic studies of ST3GAL3 revealed a strong preference for lactotetraosylceramide as acceptor, and gangliotetraosylceramide was also efficiently utilized in vitro. Moreover, the p.A13D missense variant, the one maintaining residual sialyltransferase activity, was found to have much lower affinity for all suitable substrates than the wild type enzyme, with an overall catalytic efficiency almost negligible. Altogether the present data suggest that the apparent redundancy of ST3GALs deduced from knock-out mouse models only partially exists in humans. In fact, our patients lacking ST3GAL3 activity synthesize the CA19.9 epitope sialyl-Lewis a, but not all glycans necessary for fine brain functions, where the role of minor gangliosides deserves further attention.

Introduction

Sialylation is a functionally crucial glycosylation step (Dall'Olio et al. 2014, Sato and Hane 2018) widely present during evolution (Teppa et al. 2016). Sialyltransferases constitute a family of genes and enzymes responsible for the addition of sialic acid to almost all glycan types. They show definite linkage specificity, and in several cases, even overlapping acceptor specificity. Cloning and expression of rat (Wen et al. 1992), human (Kitagawa and Paulson 1993) and mouse (Kono et al. 1997) ST3GAL3 cDNA indicated that saccharides terminating with the Gal β 1,3GlcNAc sequence, known as the type 1 chain, were the preferred substrates, although type 2 chain saccharides, terminating with the Gal β 1,4GlcNAc sequence, were also utilized. Conversely, gangliotetraosylceramide (asialo-GM1, Gal β 1,3GalNAc β 1,4Gal β 1,4Glc-Cer) was not utilized by the mouse enzyme, and other saccharides terminating with the Gal β 1,3GalNAc sequence appeared as rather poor acceptors (Gupta et al. 2016). ST3GAL3 mRNA was found to be widely expressed in rodent and human tissues, including the brain. Based on transfection studies in human gastric cancer cell lines, ST3GAL3 was proposed to be necessary for the synthesis of sLea, the sialyl-Lewis a tetrasaccharide (Sia α 2,3Gal β 1,3[Fuc β 1,4]GlcNAc) (Carvalho et al. 2010, Gomes et al. 2013), epitope of the CA19.9 antigen, a putative biomarker widely used for clinical applications (Trinchera et al. 2017). More recently, double KO mice for both st3gal2 and st3gal3 were found to lack gangliosides GD1a and GT1b in the brain, while the corresponding single KO mice were not (Sturgill et al. 2012). This suggested that mouse st3gal3 is able to use GM1 as an acceptor in vivo. Noteworthy, st3gal3 KO mice presented only minor hematologic abnormalities (Ellies et al. 2002, Kiwamoto et al. 2014). In 2011 (Hu et al. 2011), differentially aged members from two Iranian families were reported to suffer from a non-syndromic intellectual disability associated with two distinct recessive missense mutations in *ST3GAL3*: c.38C>A and c.1108G>T (p.A13D and p.D370Y, respectively). Successively (Edvardson et al. 2013), two sibling children diagnosed with West syndrome evolving to Lennox-Gestaut syndrome were found to carry another recessive missense mutation of the gene, c.958C>G (p.A320P). Variants p.A320P and p.D370Y were found to abolish enzyme activity and to impair protein metabolism and intracellular localization, while the p.A13D variant retained substantial enzyme activity and partially correct Golgi localization.

Here, we report a novel ST3GAL3 variant discovered in two infant twin siblings, presenting a picture of epileptic encephalopathy with impaired neuromotor development. To characterize the variant, we cloned and expressed the cDNA to determine the enzyme activity in vitro, by direct enzyme assay, and the protein expression by western blotting. We also prepared a tagged version of the variant to determine the subcellular localization through confocal microscopy. To assess the pathogenetic role of the loss of function of ST3GAL3, we measured the levels of CA19.9 circulating in the patient serum and determined the enzyme kinetics toward various acceptor substrates.

Results

Detection of a novel non-sense ST3GAL3 variant

The probands were two twin siblings, 18 months old: a male and a female born from a spontaneous dichorionic di-amniotic pregnancy to a healthy and apparently non consanguineous couple, whose family history was unremarkable. The pregnancy was uneventful, and no prenatal genetic tests had been performed. The twins were born at 37 weeks of gestation by caesarean section.

Patient 1. The boy's birth weight was 2905 g (25-50th centile). The Apgar scores were 2 at the 1st, 8 at the 5th minute, and 9 at the 10th minute. At birth, oxygen and tactile stimulation were required, with prompt resumption of vital parameters. In the first months of life, the baby showed normal growth parameters and a slight neuromotor delay, with head control reached at 4 months.

At 7 months of life, several episodes of brief (a few seconds) psychomotor arrest with ocular deviation were noted, increasing with frequency from 2-3 to 5-6 episodes/day, so electroencephalography (EEG) was performed, which showed diffuse epileptiform discharge during the phase of falling asleep. Neurologic evaluation showed posterior plagiocephaly with normal occipitofrontal circumference (25-50th centile), motor hyperkinesia, and mild psychomotor delay, with symmetric but not fluent spontaneous motility, and incomplete control of the trunk. The baby did not show evident dysmorphisms and underwent several diagnostic procedures (blood tests, abdominal and cardiac ultrasound, eye evaluation, and plasmatic and urinary organic acid dosage) that provided normal results. A further EEG recorded frontal sharp and spike epileptiform anomalies, both isolated and organized in sequences. Concurrently, with a clinical episode of clonus of the head and upper limbs, EEG showed the organization of the anomalies in a rhythmic and hypersynchronous sequence.

Valproate antiepileptic therapy was set up with increasing dosage up to 26 mg/kg/day, with incomplete control of fits, then ethosuximide was added with increasing dosage up to 23 mg/kg/day, but, despite this, the patient showed up to 10 fits/day.

A brain magnetic resonance was performed, and diffusion weighted imaging showed diffusivity restriction at periaqueductal and posterior region of the pons, at the mesencephalic region, and at middle cerebellar peduncles, with corresponding T2 hyperintensity. No spike anomalies were present according to MRI spectroscopy. At 18 months the baby showed generalized hypotonia with a slight improvement of motor skills; as he kept autonomous sitting posture, he rolled and crawled. Language was limited to modulated vocalizations. He still had about 2 fits/day, despite progressive increased dosage of antiepileptic therapy, up to 42 mg/kg/day of valproate and 28 mg/kg/day of ethosuximide.

Patient 2. The girl's birth weight was 2475 g (25th centile). The Apgar scores were 7 at the 1st and 9 at the 5th minute. The neonatal period was physiological. In the first months of life, the baby showed normal growth

parameters and a slight neuromotor delay with head control reached at 4 months; hyper-excitability was also observed.

At 8 months of life, several fit episodes similar to those of the brother were noted, and EEG showed diffuse polymorphic epileptiform abnormalities. Various diagnostic procedures, including brain magnetic resonance and neurologic evaluation, overlapped with those of the brother, with associated slight hyper-excitability.

Valproate antiepileptic therapy was set up with increasing dosage up to 26 mg/kg/day, with good initial control of the fits. At 12 months of life, due to recurrence of epileptic episodes, the valproate dosage was progressively increased up to 36 mg/kg/day, and ethosuximide was added up to 24 mg/kg/day, with clinical improvement. At 18 months of life, she had no residual fits. She showed generalized hypotonia with a slight improvement of motor skills; as she kept an autonomous sitting posture, she rolled and crawled. Some motor stereotypies have been observed. Language was limited to modulated vocalizations.

At the age of 10 months, a whole exome sequencing analysis was performed on the probands and their parents, and a homozygous variant of the *ST3GAL3* gene was identified in both twins, Chr1(GRCh38.p13 NC_000001.11): g.43899643C>A; NM_006279: c.660C>A; NP_006270.1: p.Tyr220ter (Y220*) (Figure 1). The parents were heterozygous carriers of the same mutation. The identified variant was confirmed by direct DNA sequencing.

Characterization of the novel c.660C>A (p.Y220) non-sense variant.*

To assess the consequences of the mutations, the pcDNA3-ST3GAL3 plasmid was mutagenized and transfected in HEK-293T cells, together with a luciferase-expressing plasmid as an internal control for normalizing transfection efficiency. Transfected cells were then processed to obtain mRNA for ST3GAL3 transcripts evaluation, cell homogenates for enzyme activity determination, and lysates for protein analysis. Expression levels of the ST3GAL3 transcript in parental or mock transfected HEK-293T cells were 16-30 thousand-fold less than GAPDH (14-15 Δ Ct), while the levels measured upon transfection became close to that of GAPDH, without relevant differences between the wild type (WT) and the variants (Figure 2A). Using the cell homogenates as the enzyme source and LNB-*p*NP (*para*-nitrophenyl-lacto-N-biose, Gal β 1,3GlcNAc β 1-O-C₆H₄NO₂) as an acceptor, sialyltransferase activity was unmeasurable in parental or mock transfected cells, while it was detectable upon transfection of the WT pcDNA3-ST3GAL3 plasmid. Enzyme activity remained, instead, undetectable upon transfection of plasmids carrying the novel p.Y220* variant, as well as p.A320P and p.D370Y variants (Figure 2A). Since WT ST3GAL3 activity was grossly proportional from 1 to 100 μ g of homogenate proteins (Figure 2B), we calculated that the residual activity in such variants, if any, should be less than 1% of the WT. Sialyltransferase activity towards LNB-*p*NP was also detectable with the p.A13D variant, which maintained about 25% of the specific activity measured with the WT construct (Figure 2A). Western blot analysis of protein lysates obtained from the same

transfectants showed that ST3GAL3 was undetectable in parental or mock transfected HEK-293T cells (Figure 2C). Upon transfection of WT ST3GAL3, a spot of about 47 kDa was visible with an antibody directed toward the N-terminal of the protein. Similar spots were evident upon transfection with p.A320P and p.D370Y variants. Conversely, upon transfection of the p.Y220* cDNA, a brighter spot of about 27 kDa was detected, confirming the expression of a truncated protein about 20 kDa smaller. Densitometric scanning of the gels indicated that the amount of this band, referred to that of β -actin, is about 8 times more abundant than that present in the WT or missense variants. Nothing was visible using the protein lysate obtained upon transfection of the p.A13D variant (Figure 2C). Since such transfectant expressed the ST3GAL3 transcript and enzyme activity, we suspected that the recognition of the N-terminus-specific antibody was impaired by the proximity of the mutation. To assess this hypothesis, we transfected Halo-tagged constructs and performed western blotting using an anti-HaloTag antibody. In this way, the p.A13D variant was detected as a spot, similar to those obtained with the WT or p.A320P and p.D370Y variants, with an apparent molecular weight (MW) of about 80 kDa (Figure 2D), as expected due to the size of the HaloTag (33 kDa). The size of the Halo-tagged p.Y220* variant was about 60 kDa, which appeared slightly accumulated with respect to the WT, as much as the missense variants. An additional spot of about 40 kDa of unknown origin was evident with the HaloTag WT construct only. We also measured the sialyltransferase activity of the cell homogenates obtained from such transfections with the HaloTag constructs and obtained results similar to those obtained with the pcDNA3 plasmids (supplementary Figure S1). No activity was detectable with the HaloTag p.Y220*, p.A320P, and p.D370Y variants, and reduced activity with the HaloTag p.A13D construct was observed, about 30% of that obtained with the HaloTag WT construct. These results corroborate the hypothesis that the p.A13D variant is not detectable by the anti-ST3GAL3 antibody used, suggesting that the mutation is relevant enough to the protein conformation to affect antigenicity. HEK-293T cells transfected with the HaloTag constructs of the WT and p.Y220* ST3GAL3 variant were also analyzed by confocal microscopy upon staining with the HaloTag specific ligand TMR and antibodies against endoplasmic reticulum (ER) and Golgi apparatus markers (Figure 3). The results showed similar co-localization of both the WT and p.Y220* variant with the Golgi apparatus marker, and minimal co-localization with the ER marker of the p.Y220* variant only, suggesting that the truncated protein is rather well transported to the site of action.

Detection of circulating CA19.9 antigen

Assuming the hypothesis that ST3GAL3 is necessary to sialylate glycoproteins carrying glycans terminating with the Gal β 1,3GlcNAc sequence (Carvalho et al. 2010, Gomes et al. 2013), as in the case of the sLea tetrasaccharide, patients lacking ST3GAL3 activity were expected to lack the circulating CA19.9 antigen. To confirm the hypothesis, patient serum was analyzed for CA19.9 expression by sandwich enzyme-linked immunosorbent assay (ELISA) and by dot-blot immunostaining. Surprisingly, both siblings were found to

express the antigen, by both techniques. In particular, the expression was higher than in the heterozygous parents and other adult controls by ELISA (Figure 4), and very similar to parents and controls by dot-blot analysis (Figure 5). These results strongly suggest that other ST3GALs efficiently rescued ST3GAL3 deficiency.

Kinetics of ST3GAL3

To better compare the functional properties of the WT and ST3GAL3 variants, activity assays were performed using various acceptors at different concentrations. To this aim, known suitable substrates were used, such as Lc4 (lactotetraosylceramide, Gal β 1,3GlcNAc β 1,3Gal β 1,4Glc-Cer), and asialo-AGP (asialo- α 1-acid glycoprotein) in addition to LNB-*p*NP. We also included the GM1 ganglioside and asialo-GM1, which bear the Gal β 1,3GalNAc terminal saccharide sequence. The results are presented in Table I, Figure 6A, and Supplementary Figure S2. Lc4 appeared as the largely preferred substrate, with an affinity 35- and 11-fold higher than asialo-AGP and asialo-GM1, respectively. Surprisingly, asialo-GM1, but not at all GM1, was efficiently used by WT ST3GAL3, with an affinity better than asialo-AGP. Properties of the p.A13D variant appear very different: activity was faintly detectable with Lc4 and asialo-AGP, while affinities for both LNB-*p*NP and asialo-GM1 were about 7-fold lower than those measured with the WT enzyme. Since the calculated *V*_{max} values were also lower, the catalytic efficiency with these acceptors is over 25-fold lower. Since the impairment with Lc4 and asialo-AGP is even worse, the data suggest that the residual activity maintained by the p.A13D ST3GAL3 variant may not be relevant *in vivo*. The other variants, including the novel p.Y220* non-sense variant, remained totally inactive, despite using these alternative substrates as acceptors.

Pathogenic variants of another sialyltransferase, ST3GAL5 (GM3 synthase), are reported to lack any detectable enzyme activity *in vitro* (Indelicato et al. 2019). Conversely, a pathogenic variant of B4GALNT1 (GM2 synthase), p.R300C (Bhuiyan et al. 2019), is reported to retain some activity. We determined the kinetics of WT B4GALNT1 and p.R300C variant, calculated upon transfecting HEK-293T cells with cDNAs in pcDNA3-based plasmids. The results showed almost identical affinity of the WT and B4GALNT1 variant for GM3, and a 35-fold lower *V*_{max} of the variant (Table I and Figure 6B). Taken together, these data suggest missense mutations are able to affect the catalytic properties of glycosyltransferase in very different ways difficult to predict on the basis of their simple position.

Discussion

In this article we described a non-sense variant of ST3GAL3 able to inactivate the enzyme as the main consequence. The variant, detected in two infant siblings was associated with clinical signs of epilepsy and neuromotor delay, compatible with the clinical features previously reported in patients carrying other ST3GAL3 variants. Our patients were found to express significant levels of circulating CA19.9 in the serum.

At present, ST3GAL3-CDG has been reported in young adults as a non-syndromic intellectual disability (p.A13D and p.D370Y variants) (Hu et al. 2011), or in children-teenagers (Edvardson et al. 2013) and babies (present article) as an epileptic encephalopathy syndrome (p.A320P and p.Y220* variants). All variants were found to inactivate the enzyme in vitro, except for p.A13D, and all were found to affect protein transport, although in a minimal or weak manner in the case of p.Y220* or p.A13D variants, respectively. The low number of cases and their heterogeneity in age of diagnosis and follow-up do not yet allow for establishing a narrow relationship between an individual mutation and clinical presentation. However, the overall data suggest that impaired function of ST3GAL3 affects fine mechanisms within the central nervous system, without involvement of other tissues and organs. Coherently, a methylome-wide study included ST3GAL3 in the epigenetic profile of attention deficit/hyperactivity disorder patients (Walton et al. 2017). Despite total inactivation of ST3GAL3, our patients express relevant amounts of the CA19.9 antigen, as detected by both ELISA and dot blotting. Since sandwich ELISA is sensitive to high MW proteins carrying multiple epitopes (as mucins), but not to smaller antigenically monovalent proteins, which are instead better detected by dot-blotting (Mare et al. 2013), we conclude that a wide spectrum of glycoproteins carrying the Gal β 1,3GlcNAc disaccharide at the terminus of their sugar chains are sialylated, even in the absence of functional ST3GAL3. The values detected in both patients by ELISA (142 and 56.5 U/ml) are higher than those found in both parents, which are within the commonly accepted range for adults (37 U/ml). This is probably due to their very young age, in which circulating CA19.9 is known to be higher and more heterogeneous than in adults (Bevilacqua et al. 2014). The reason why age-dependent CA19.9 elevation is detected by ELISA and not by dot-blotting is not known, and we suggest that this depends on the carrier molecules rather than on the sLea epitope. At present, it is not possible to predict which ST3GAL is able to drive the synthesis of CA19.9 in the absence of ST3GAL3. Data obtained in recombinant gastric cell lines suggest ruling out ST3GAL4 (Carvalho et al. 2010, Gomes et al. 2013), but no data are available for the other members of the family. Our data showed that human ST3GAL3 strongly prefers use of Lc4 as an acceptor, forming sialyl-Lc4 (Sia α 2,3Gal β 1,3GlcNAc β 1,3Gal β 1,4Glc-Cer), a ganglioside of the lacto-series, originally named 3'isoLM1 (Nilsson et al. 1985). Sialyl-Lc4 was found to be a very minor component of infant brain gangliosides (Molin et al. 1987). Due to its very low concentration, about 40 and 400 times less than GM2 and GM1, respectively, the potential role of such ganglioside has never been studied in the brain. However, the reported quantitation refers to the whole brain, while such molecule may be specific for particular cells or areas of the brain, as suggested by successive reports (Fredman et al. 1993). Moreover, the good catalytic efficiency of human ST3GAL3 with asialo-GM1 confirms the particular preference of the enzyme for the ceramide moiety, which is able to make the unfavorable Gal β 1,3GalNAc disaccharide sequence a suitable acceptor. In this context, the specific lack of sialyl-Lc4 may be relevant in the pathogenesis of ST3GAL3-CDG. Recently, cortical neurons differentiated from induced pluripotent stem cells obtained from a patient carrying the p.A320P variant were found to have very minimal effects in the

α 2,3 sialylation pattern of glycoproteins, as detected by *Maackia Amurensis* staining of western blots (van Diepen et al. 2018). This is compatible with the hypothesis of an involvement of gangliosides in the disease. On the other hand, it is also possible that ST3GAL3 specifically acts on a subset of glycoproteins carrying the Gal β 1,3/4GlcNAc or even Gal β 1,3GalNAc sequence, or both, unknown at present and exclusively expressed in dedicated cells of the brain.

We have found that the p.A13D variant, the only ST3GAL3 pathogenic variant maintaining residual sialyltransferase activity, has very low catalytic efficiency with several substrates, including Lc4, asialo-AGP, and asialo-GM1. In this light, it is strongly possible that the residual activity of the enzyme is just detectable in vitro at saturating acceptor concentrations, which are not functionally relevant, thus suggesting that all pathogenic variant causing a congenital disorder of glycosylation are responsible for a lack of specific sialylation in vivo. Our findings indicated that this ST3GAL3 variant affects the K_m more than the V_{max} , while the p.R300C B4GALNT1 variant dramatically impairs the V_{max} only.

In our cell model, ST3GAL3 variants appear efficiently expressed, as deduced by western blot analysis. The predicted MW of the whole protein and of the truncated Y220* variant is about 42 and 24.5 kDa, respectively, while they appear a little heavier by western blotting, suggesting that they are probably glycosylated. Upon transfection in pcDNA3-based plasmid and detection by western blotting using the anti-ST3GAL3 antibody, the novel non-sense variant **was** significantly accumulated. Conversely, upon transfection in pFN21A-based plasmid and detection by anti-HaloTag antibody, the levels of Halo tagged ST3GAL3 remained similar to those found with the missense variants. It is possible that the truncation affected conformation and antigenicity, or even that the chimera underwent a different turn-over. Consequently, a definitive conclusion about Y220* variant accumulation can not be drawn. An additional band of about 40 kDa was present with the Halo tagged WT ST3GAL3 construct. Due to its small size, it should be mainly constituted by the HaloTag. The native ST3GAL3 gene is known to undergo multiple splicing (Grahn et al. 2003, 2004), giving rise to several inactive short proteins, but this appears unlikely with our plasmid construct, and we are unable to explain its differential origin. Taken together, our data suggest that loss of activity is crucial in ST3GAL3-CDG, although other concomitant events due to altered proteostasis could play a role. In fact, p.A320P and p.D370Y variants are reported to be retained in the ER, and we found that even the novel p.Y220* variant, which is almost properly transported to the Golgi apparatus, may be accumulated when expressed in HEK-293T. Moreover, p.Y220* truncation, causing the catalytic domain to be lost soon after the large sialyl motif, and p.A320P mutation, located inside the short sialyl motif, are both associated to epileptic encephalopathy. p.A13D and p.D370Y mutations, which are located far from the sialyl motifs, are both associated to intellectual disability only. KO of single glycosyltransferase in the mouse frequently provides almost normal phenotypes (Trinchera et al. 2018), and double KO is thus necessary for relevant phenotypic alterations because of the overlapping specificity of members of large gene families. This was also the case of mouse *st3gal3* (Ellies et al. 2002, Kiwamoto et

al. 2014, Sturgill et al. 2012). Our data suggest that such an apparent redundancy of **sialyltransferases** exists in humans only for some glycosylations, as those responsible for sLea biosynthesis. Conversely, the complexity of human brain glycome requires **the action of individual members of the sialyltransferase family**.

Materials and methods

Genomic DNA analysis

After genetic counselling and written informed consent, genomic DNAs of patients and both parents were extracted, processed and analyzed as previously reported (Indellicato et al. 2019).

Materials

Gangliosides GM1 and GM3 were available as reported (Trinchera and Ghidoni 1989). LNB-*p*NP (lacto-N-biose-*p*NP, Gal β 1,3GlcNAc β 1-O-C₆H₄NO₂) was from Tokyo Chemical industry (G0420) and asialo-AGP (asialo- α 1 acid-glycoprotein) was prepared by mild acid hydrolysis (50 mM H₂SO₄, 80 °C, 1h), followed by exhaustive dialysis against water (Dall'Olio et al. 2006). Asialo-GM1 and Lc4 were prepared as detailed under Supplementary Methods. Anti-ST3GAL3 antibody was purchased from Sigma (AV46706, Lot: QC16795) and used at 1:1000 dilution.

DNA constructs and transfections

ST3GAL3 coding sequence was amplified by PCR using cDNA prepared by reverse transcription of RNA extracted from Human brain (Clontech) in the presence of FidelityTaq DNA polymerase (Affymetrix #71180) according to the manufacturer's protocol and using the reported primer pair (Supplementary Table S1). Amplification was for 30 cycles and annealing temperature 64°C. The obtained cDNA was purified (Wizard SV Gel and PCR Clean-Up system, Promega), digested with *Hind*III and *Xba*I (sites added in the primer sequences) and cloned in the corresponding sites of pcDNA3 vector. Plasmid inserts were **then** submitted to direct DNA sequencing to assess fidelity and were found to correspond to the B1 transcript described by Grahm et al. (2003).

B4GALNT1 coding sequence was amplified by PCR as reported for ST3GAL5 (Indellicato et al. 2019). Amplification was for 30 cycles and annealing temperature 67.5°C. The primer pair used is reported in Supplementary Table S1. The obtained cDNA was cloned as above described for ST3GAL3. pcDNA3-ST3GAL3 and pcDNA3-B4GALNT1 were mutated using the reported primer pairs (Supplementary Table S1) according to our previous report (Indellicato et al. 2019), as detailed under Supplementary Methods. WT and mutated pcDNA3-ST3GAL3 plasmids were digested with *Sgf*I and *Pme*I (sites added to the primer

sequences, see Supplementary Table S1) and cloned in the corresponding sites of pFN21A vector (Promega). This allows to place the coding sequences in frame with the HaloTag.

HEK-293T cells were transiently transfected with a mixture of expression plasmids (either in pcDNA3 or pFN21A-HaloTag) and luciferase reporter plasmid as reported (Zulueta et al. 2014). One tenth aliquot was resuspended with 25 μ l of passive lysis buffer (Promega) for luciferase assay, and the remaining part divided in 2 aliquots, one resuspended with 0.1 M Tris/HCl pH 7.4 containing 0.1% Triton-X100 for enzyme assay, another with RIPA buffer for western blotting (Indelicato et al. 2019).

Enzyme assay

For B4GALNT1 assay, the reaction mixture contained, in a final volume of 0.03 ml, 0.2 M Tris/HCl buffer pH 7.0, 10 mM $MnCl_2$, 5 mM CDP-Choline, 0.2 mM UDP-[3H]GalNAc (specific activity 5-10 mCi/mmol), 0.2% Triton-X100, various concentrations of GM3, and various amounts of cell homogenate as the enzyme source (see results). For kinetic studies, 5.0 and 90 μ g of homogenate proteins were used for the WT and p.R300C variant, respectively. For ST3GAL3 assay, the reaction mixture contained, in a final volume of 0.015 ml, 0.2 M Cacodylate/HCl buffer pH 6.5, 0.2 mM CMP-[3H]Sia (specific activity 5-10 mCi/mmol), 0.2% Triton-X100, and various concentrations of acceptors and cell homogenates (see results). For kinetic studies, 20 and 70 μ g of homogenate proteins were used for the WT and p.A13D variant, respectively. Blanks were regularly prepared by omitting the acceptors in the reaction mixture and sometimes preparing identical mixtures containing cell homogenates from parental HEK-293T as the enzyme source. Glycosphingolipid acceptors and detergent, or the detergent alone in the blanks, were dissolved in chloroform/methanol, 2:1 (vol/vol), placed in the reaction tubes and allow to dry overnight before adding the other reaction components. LNB-*p*NP was dissolved in methanol alone and then mixed with detergent and dried as for glycosphingolipids. Samples were incubated at 37 °C for 1 h. In the case of glycosphingolipid acceptors, the mixture was spotted on Whatman 3MM paper and assayed by descending chromatography in 1% tetraborate (Salvini et al. 2001). The radioactivity of the appropriate areas was measured by liquid scintillation using 5 ml of Instagel (Packard) and the blank values subtracted. In that of LNB-*p*NP, the reaction mixture was diluted to 1 ml with water, loaded onto a Sep-Pack C18 cartridge previously equilibrated with methanol, rinsed with 5 ml of water, and eluted with 2 ml of methanol. The methanolic fraction was dried and submitted to liquid scintillation counting as above. Reactions with asialo-AGP as acceptor were assayed as reported (Dall'Olio et al. 2006). Luciferase was assayed as previously reported (Mare and Trinchera 2007) using 1 μ l of a 1:20 dilution in passive lysis buffer of the cell lysate obtained as above described, and 25 μ l of Firefly luciferase assay reagent I (Promega). Protein concentration was determined using a BCA assay kit (Pierce).

Detection of CA19.9 in patient serum

Patient serum was prepared from blood residual after a collection performed for care reasons. For dot blotting, serum was diluted with water in order to have 1 μ l in 80 μ l and then serially diluted with water to 1:64. Aliquots (80 μ l) were applied to a blotter (Bio-Rad) for absorption on a nitrocellulose membrane, which was washed and processed for anti CA19.9 staining as reported (Aronica et al. 2017).

Chemiluminescence detection was performed as reported (Indellicato et al. 2019). ELISA were performed in 96 well plates (Nunc F8 Maxisorp Immuno-module) which were covered (4°C overnight) with 0.1 ml of anti CA19.9 antibody, 4 mg/ml in Tris buffer 0.2 M pH 9.4, blocked with 0.2 ml FBS, and allow to react with 0.1 ml of human serum, 1h at RT. Plates were washed 3 times with PBS-T (phosphate buffered saline containing 0.1% Tween-20) and detected with peroxidase-labeled anti CA19.9 antibody (1:5000), 75 min at RT. After washing 5 times with PBS-T, the reactions were developed using 0.1 ml TMB (Sigma), 5-20 min at RT, and stopped with 0.1 ml 1N HCl. The resultant colors were evaluated in a microtiter plate reader. Calibration standards were from CanAg CA19.9 kit (Fujirebio). Peroxidase-labeled antibody for detection was prepared starting from anti-CA19.9, 2.5 mg/ml, double purified by protein-A Sepharose chromatography, and using Lightning-Link® HRP Conjugation Kit (Innova Biosciences), according to the manufacture's protocol. Anti-CA19.9 monoclonal antibody was purified from the culture medium of hybridoma NS-1116-19-9 (ATCC HB-8059) by ammonium sulfate precipitation and affinity chromatography on a Protein A Sepharose column. Other analytical procedures were according to our published protocols (Aronica et al. 2017, Indellicato et al. 2019) as detailed under Supplementary Methods.

Acknowledgments

The authors wish to thank the patient's parents who agreed with the publication of clinical data and the use of the serum residual from clinical collection. We also thank Daniele Bottai (University of Milan) for the help with microscopy slide preparation. The following institutions supported the paper: Università dell'Insubria, Fondo Ateneo Ricerca 2018 (to MT), Ministero dell'Università e della Ricerca scientifica e tecnologica, *Fondo per il finanziamento delle attività base di ricerca* 2017 (to MT). PhD program in Translational Medicine of the University of Milan (to RI). The authors declared no conflict of interest.

Abbreviations

Glycosyltransferases are named according to the HUGO recommendations.

asialo-AGP, asialo- α_1 -acid glycoprotein; asialo-GM1, gangliotetraosylceramide, Gal β 1,3GalNAc β 1,4Gal β 1,4Glc-Cer; ER, endoplasmic reticulum; LNB-*p*NP, *para*-nitrophenyl-lacto-N-biose, Gal β 1,3GlcNAc β 1-O-C₆H₄NO₂); EEG, electroencephalography; ELISA, enzyme-linked immunosorbent assay; Lc4, lactotetraosylceramide, Gal β 1,3GlcNAc β 1,3Gal β 1,4Glc-Cer; MW, molecular weight; sLea, sialyl-Lewis a, Sia α 2,3Gal β 1,3[Fuc β 1,4]GlcNAc; WT, wild-type.

References

- Aronica A, Avagliano L, Caretti A, Tosi D, Bulfamante GP, Trinchera M. 2017. Unexpected distribution of CA19.9 and other type 1 chain Lewis antigens in normal and cancer tissues of colon and pancreas: Importance of the detection method and role of glycosyltransferase regulation. *Biochimica et biophysica acta. General subjects*, 1861:3210-3220.
- Bevilacqua V, Chan MK, Chen Y, Armbruster D, Schodin B, Adeli K. 2014. Pediatric population reference value distributions for cancer biomarkers and covariate-stratified reference intervals in the CALIPER cohort. *Clinical chemistry*, 60:1532-1542.
- Bhuiyan RH, Ohmi Y, Ohkawa Y, Zhang P, Takano M, Hashimoto N, Okajima T, Furukawa K. 2019. Loss of Enzyme Activity in Mutated B4GALNT1 Gene Products in Patients with Hereditary Spastic Paraplegia Results in Relatively Mild Neurological Disorders: Similarity with Phenotypes of B4galnt1 Knockout Mice. *Neuroscience*, 397:94-106.
- Carvalho AS, Harduin-Lepers A, Magalhaes A, Machado E, Mendes N, Costa LT, Matthiesen R, Almeida R, Costa J, Reis CA. 2010. Differential expression of alpha-2,3-sialyltransferases and alpha-1,3/4-fucosyltransferases regulates the levels of sialyl Lewis a and sialyl Lewis x in gastrointestinal carcinoma cells. *The international journal of biochemistry & cell biology*, 42:80-89.
- Dall'Olio F, Malagolini N, Chiricolo M. 2006. Beta-galactoside alpha2,6-sialyltransferase and the sialyl alpha2,6-galactosyl-linkage in tissues and cell lines. *Methods Mol Biol*, 347:157-170.
- Dall'Olio F, Malagolini N, Trinchera M, Chiricolo M. 2014. Sialosignaling: sialyltransferases as engines of self-fueling loops in cancer progression. *Biochimica et biophysica acta*, 1840:2752-2764.
- Edvardson S, Baumann AM, Muhlenhoff M, Stephan O, Kuss AW, Shaag A, He L, Zenvirt S, Tanzi R, Gerardy-Schahn R, et al. 2013. West syndrome caused by ST3Gal-III deficiency. *Epilepsia*, 54:e24-27.
- Ellies LG, Sperandio M, Underhill GH, Yousif J, Smith M, Priatel JJ, Kansas GS, Ley K, Marth JD. 2002. Sialyltransferase specificity in selectin ligand formation. *Blood*, 100:3618-3625.
- Fredman P, von Holst H, Collins VP, Dellheden B, Svennerholm L. 1993. Expression of gangliosides GD3 and 3'-isoLM1 in autopsy brains from patients with malignant tumors. *Journal of neurochemistry*, 60:99-105.
- Gomes C, Osorio H, Pinto MT, Campos D, Oliveira MJ, Reis CA. 2013. Expression of ST3GAL4 leads to SLe(x) expression and induces c-Met activation and an invasive phenotype in gastric carcinoma cells. *PLoS one*, 8:e66737.

- Grahn A, Barkhordar GS, Larson G. 2003. Cloning and sequencing of nineteen transcript isoforms of the human alpha2,3-sialyltransferase gene, ST3Gal III; its genomic organisation and expression in human tissues. *Glycoconjugate journal*, 19:197-210.
- Grahn A, Barkhordar GS, Larson G. 2004. Identification of seven new alpha2,3-sialyltransferase III, ST3Gal III, transcripts from human foetal brain. *Glycoconjugate journal*, 20:493-500.
- Gupta R, Matta KL, Neelamegham S. 2016. A systematic analysis of acceptor specificity and reaction kinetics of five human alpha(2,3)sialyltransferases: Product inhibition studies illustrate reaction mechanism for ST3Gal-I. *Biochemical and biophysical research communications*, 469:606-612.
- Hu H, Eggers K, Chen W, Garshasbi M, Motazacker MM, Wrogemann K, Kahrizi K, Tzschach A, Hosseini M, Bahman I, *et al.* 2011. ST3GAL3 mutations impair the development of higher cognitive functions. *American journal of human genetics*, 89:407-414.
- Indelicato R, Parini R, Domenighini R, Malagolini N, Iascone M, Gasperini S, Masera N, dall'Olio F, Trinchera M. 2019. Total loss of GM3 synthase activity by a normally processed enzyme in a novel variant and in all ST3GAL5 variants reported to cause a distinct congenital disorder of glycosylation. *Glycobiology*, 29:229-241.
- Kitagawa H, Paulson JC. 1993. Cloning and expression of human Gal beta 1,3(4)GlcNAc alpha 2,3-sialyltransferase. *Biochemical and biophysical research communications*, 194:375-382.
- Kiwamoto T, Brummet ME, Wu F, Motari MG, Smith DF, Schnaar RL, Zhu Z, Bochner BS. 2014. Mice deficient in the St3gal3 gene product alpha2,3 sialyltransferase (ST3Gal-III) exhibit enhanced allergic eosinophilic airway inflammation. *The Journal of allergy and clinical immunology*, 133:240-247 e241-243.
- Kono M, Ohyama Y, Lee YC, Hamamoto T, Kojima N, Tsuji S. 1997. Mouse beta-galactoside alpha 2,3-sialyltransferases: comparison of in vitro substrate specificities and tissue specific expression. *Glycobiology*, 7:469-479.
- Mare L, Caretti A, Albertini R, Trinchera M. 2013. CA19.9 antigen circulating in the serum of colon cancer patients: where is it from? *The international journal of biochemistry & cell biology*, 45:792-797.
- Mare L, Trinchera M. 2007. Comparative analysis of retroviral and native promoters driving expression of beta1,3-galactosyltransferase beta3Gal-T5 in human and mouse tissues. *The Journal of biological chemistry*, 282:49-57.
- Molin K, Mansson JE, Fredman P, Svennerholm L. 1987. Sialosyllactotetraosylceramide, 3'-isoLM1, a ganglioside of the lactotetraose series isolated from normal human infant brain. *Journal of neurochemistry*, 49:216-219.
- Nilsson O, Mansson JE, Lindholm L, Holmgren J, Svennerholm L. 1985. Sialosyllactotetraosylceramide, a novel ganglioside antigen detected in human carcinomas by a monoclonal antibody. *FEBS letters*, 182:398-402.

- Salvini R, Bardoni A, Valli M, Trinchera M. 2001. beta 1,3-Galactosyltransferase beta 3Gal-T5 acts on the GlcNAc beta 1-->3Gal beta 1-->4GlcNAc beta 1-->R sugar chains of carcinoembryonic antigen and other N-linked glycoproteins and is down-regulated in colon adenocarcinomas. *The Journal of biological chemistry*, 276:3564-3573.
- Sato C, Hane M. 2018. Mental disorders and an acidic glycan-from the perspective of polysialic acid (PSA/polySia) and the synthesizing enzyme, ST8SIA2. *Glycoconjugate journal*, 35:353-373.
- Sturgill ER, Aoki K, Lopez PH, Colacurcio D, Vajn K, Lorenzini I, Majic S, Yang WH, Heffer M, Tiemeyer M, *et al.* 2012. Biosynthesis of the major brain gangliosides GD1a and GT1b. *Glycobiology*, 22:1289-1301.
- Teppa RE, Petit D, Plechakova O, Cogez V, Harduin-Lepers A. 2016. Phylogenetic-Derived Insights into the Evolution of Sialylation in Eukaryotes: Comprehensive Analysis of Vertebrate beta-Galactoside alpha2,3/6-Sialyltransferases (ST3Gal and ST6Gal). *International journal of molecular sciences*, 17.
- Trinchera M, Aronica A, Dall'Olio F. 2017. Selectin Ligands Sialyl-Lewis a and Sialyl-Lewis x in Gastrointestinal Cancers. *Biology*, 6.
- Trinchera M, Ghidoni R. 1989. Two glycosphingolipid sialyltransferases are localized in different sub-Golgi compartments in rat liver. *The Journal of biological chemistry*, 264:15766-15769.
- Trinchera M, Parini R, Indelicato R, Domenighini R, dall'Olio F. 2018. Diseases of ganglioside biosynthesis: An expanding group of congenital disorders of glycosylation. *Molecular genetics and metabolism*, 124:230-237.
- van Diepen L, Buettner FFR, Hoffmann D, Thiesler CT, von Bohlen Und Halbach O, von Bohlen Und Halbach V, Jensen LR, Steinemann D, Edvardson S, Elpeleg O, *et al.* 2018. A patient-specific induced pluripotent stem cell model for West syndrome caused by ST3GAL3 deficiency. *European journal of human genetics : EJHG*, 26:1773-1783.
- Walton E, Pingault JB, Cecil CA, Gaunt TR, Relton CL, Mill J, Barker ED. 2017. Epigenetic profiling of ADHD symptoms trajectories: a prospective, methylome-wide study. *Molecular psychiatry*, 22:250-256.
- Weinstein J, de Souza-e-Silva U, Paulson JC. 1982. Sialylation of glycoprotein oligosaccharides N-linked to asparagine. Enzymatic characterization of a Gal beta 1 to 3(4)GlcNAc alpha 2 to 3 sialyltransferase and a Gal beta 1 to 4GlcNAc alpha 2 to 6 sialyltransferase from rat liver. *The Journal of biological chemistry*, 257:13845-13853.
- Wen DX, Livingston BD, Medzihradszky KF, Kelm S, Burlingame AL, Paulson JC. 1992. Primary structure of Gal beta 1,3(4)GlcNAc alpha 2,3-sialyltransferase determined by mass spectrometry sequence analysis and molecular cloning. Evidence for a protein motif in the sialyltransferase gene family. *The Journal of biological chemistry*, 267:21011-21019.
- Zulueta A, Caretti A, Signorelli P, Dall'olio F, Trinchera M. 2014. Transcriptional control of the B3GALT5 gene by a retroviral promoter and methylation of distant regulatory elements. *FASEB journal : official publication of the Federation of American Societies for Experimental Biology*, 28:946-955.

Legend to figures.

Figure 1. Schematic representation of ST3GAL3 mutations in both cDNA and protein sequences. Dotted lines represent the untranslated sequences of exons 1 and 12. Exons are according to the B1 transcript reported by Grahn et al. (2003) and correspond to transcript variant 10 of GenBank (accession number NM_006279.5). L, S, 3, and VS indicate large, short, 3, and very short sialyl motifs, respectively. p.Y220* truncation and p.A320P mutation are both associated to epileptic encephalopathy; p.A13D and p.D370Y mutations are both associated to intellectual disability.

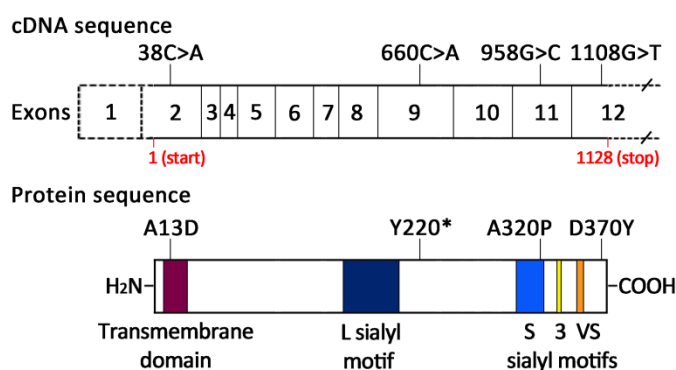


Figure 2. Characterization of the ST3GAL3 Y220* variant. HEK-293T cells were transiently co-transfected with ST3GAL3 and luciferase expression plasmids and processed to obtain cell homogenates for enzyme assay, lysates for RNA extraction, and lysates for protein analysis. Results obtained with parental cells were undistinguishable from those obtained with mock transfected cells, which were not presented. (A) Upon transfection of pcDNA3-based plasmids carrying wild type (WT) or variant ST3GAL3, cDNA synthesized from parental or transfected cells was analyzed by real-time PCR for ST3GAL3 expression using GAPDH as a reference, and the amount of ST3GAL3 transcript was calculated as $2^{-\Delta Ct}$. Homogenates from the same cells were used as the enzyme source for the detection of luciferase activity or sialyltransferase activity towards LNB-*p*-NP (1 mM). Twenty (WT) or 40 μ g (variants) of homogenate proteins were used. Results are expressed as the ratio of ST3GAL3 specific activity and luciferase activity, which is expressed as arbitrary units and acts as an internal control for normalizing transfection efficiency. One unit of luciferase activity corresponds to the luminometer measures obtained with 100 pg of protein homogenates. Results are the mean \pm SD for duplicate assays performed on two independent transfections. (B) The same homogenates as in A were used for the ST3GAL3 activity assay, but the amount of homogenate proteins was varied. Results are the mean \pm SD for duplicate assays performed on two independent transfections. (C) Membrane proteins obtained from the same cells as in A and B were solubilized with RIPA buffer, separated by 12% SDS PAGE, and blotted onto a nitrocellulose membrane that was stained with rabbit anti-ST3GAL3 antibody followed by peroxidase-labeled secondary antibody. After stripping, the membrane was

also stained with a monoclonal anti- β -actin antibody followed by peroxidase-labeled secondary antibody. The anti-ST3GAL3 antibody detected some unspecific bands present in the parental cell line. Several western blots were performed starting from 3 independent transfections and loading various amounts of lysate protein, and overlapping results were obtained. The blot presenting the best signal to background ratio is shown. (D) HEK-293T cells were transfected with pFN21A-based plasmids, which drive expression of ST3GAL3 cDNAs as fusion proteins with HaloTag. Western blotting was performed as in C but using the anti-HaloTag antibody instead of the anti-ST3GAL3 antibody. The additional band with an apparent MW of about 40 kDa, detected in the WT construct was constantly present in duplicate western blots performed with protein lysates obtained from 3 independent transfections.

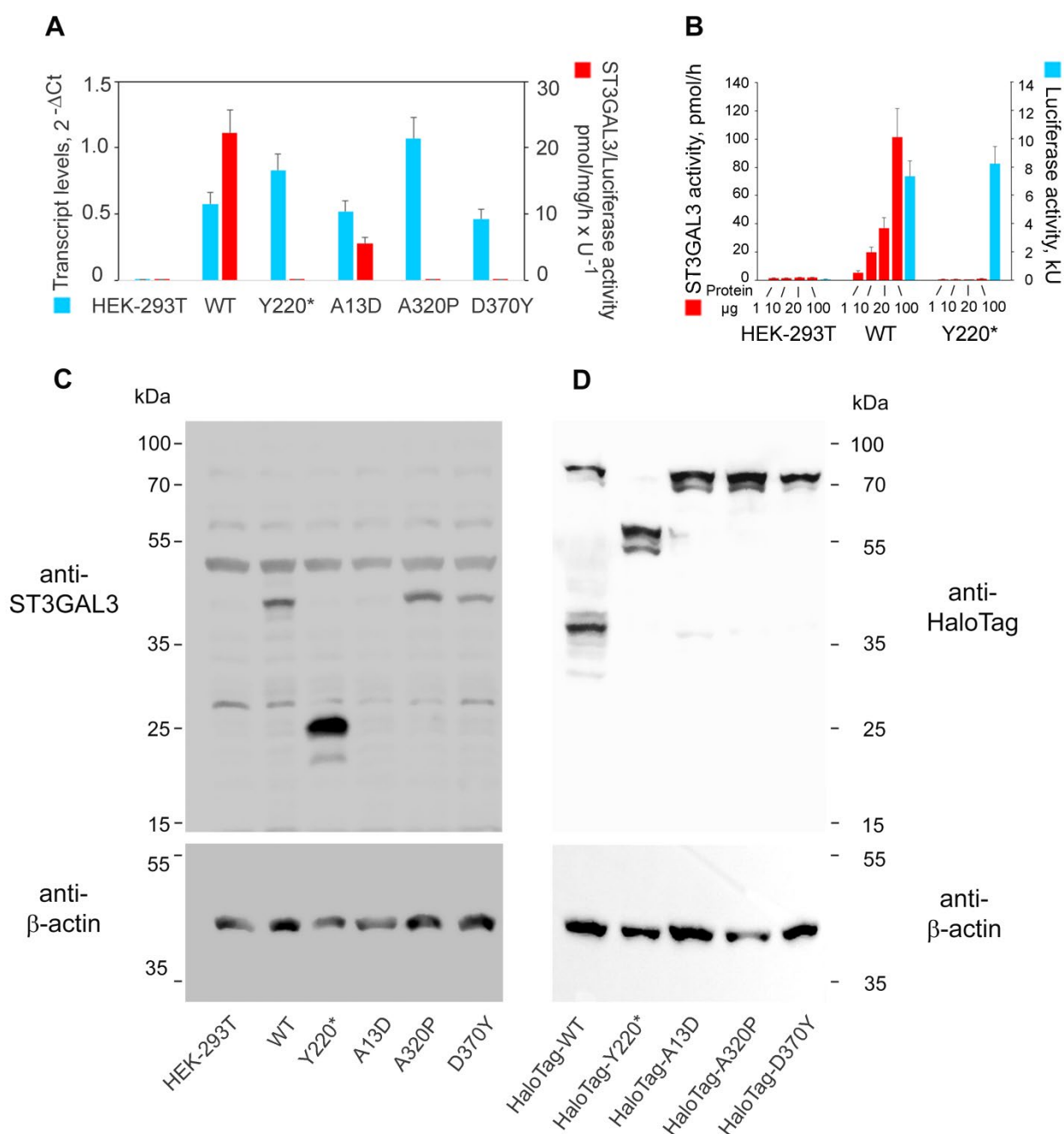


Figure 3. Confocal microscopy analysis of HEK-293T expressing the WT or Y220* variant of HaloTag-ST3GAL3 constructs. HEK-293T cells were seeded on coverslips and transiently transfected with pNF21A-based plasmids expressing the WT or Y220* variant of ST3GAL3 in frame with HaloTag. Cells were then stained with the HaloTag specific ligand TMR, fixed, permeabilized and then incubated with the anti-Golgin97 antibody (Golgi apparatus marker) or anti-PDI antibody (protein disulfide isomerase, endoplasmic reticulum marker), followed by a secondary FITC-labeled antibody. Coverslips were mounted on glass slide and analyzed by confocal microscopy. Scale bar is 10 μ m.

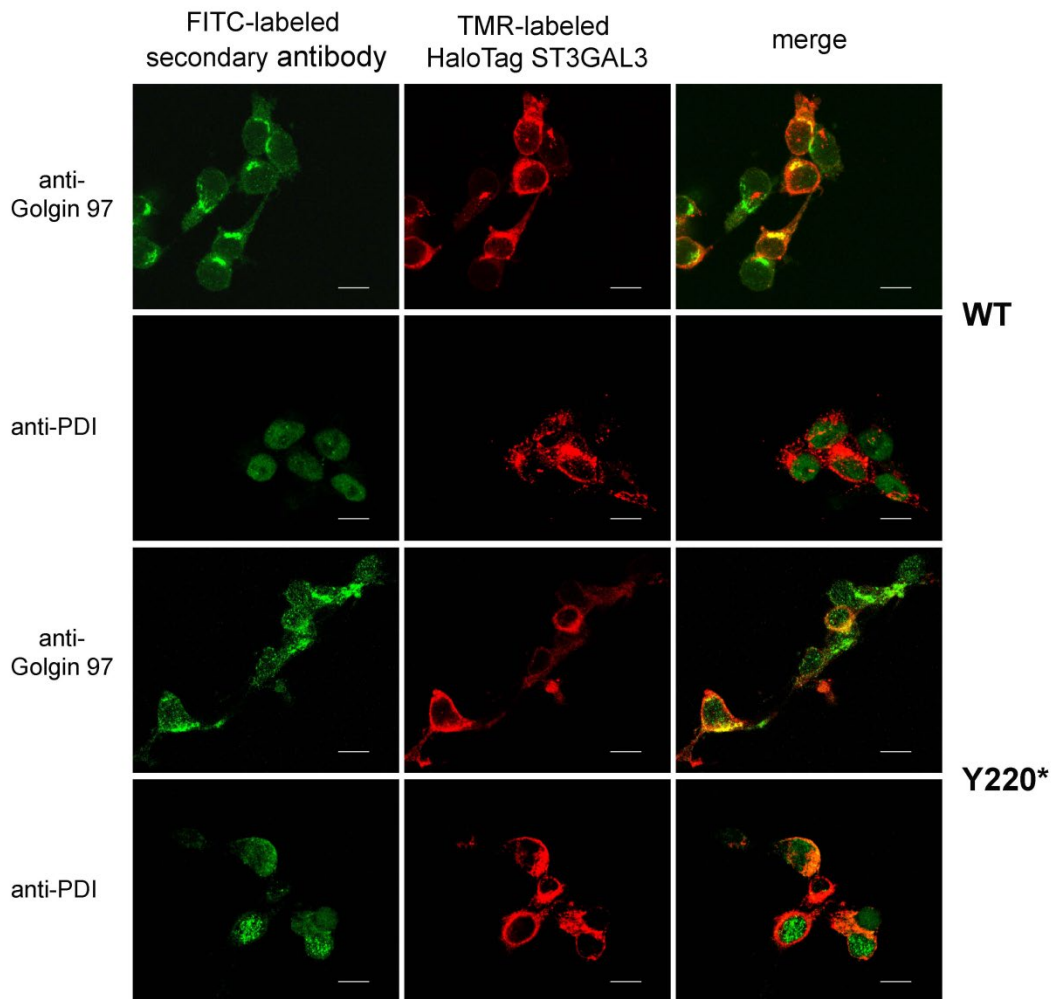


Figure 4. Detection of CA19.9 in patient serum by ELISA. Hundred microliter aliquots of serum from patients, parents, and healthy adult controls were applied to a microtiter plate prepared to perform a sandwich ELISA with anti-CA19.9 antibody as capturing and detection antibodies. Known amounts of antigen were applied in parallel for quantitation. Results are the mean for duplicate assays performed twice on a serum aliquot obtained from a single blood collection. FBS, fetal bovine serum.

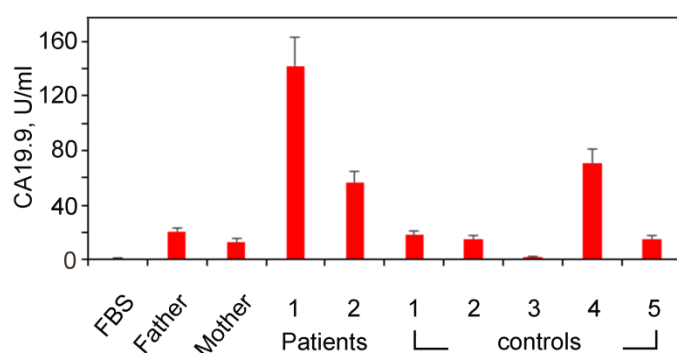


Figure 5. Detection of CA19.9 in patient serum by dot blotting. Ten μ l of serum were brought to 800 μ l with water, and serial dilutions were performed. Eighty μ l of each sample were blotted onto a nitrocellulose membrane that was stained with anti-CA19.9 antibody followed by peroxidase-labeled secondary antibody. Detection was by chemiluminescence. FBS, fetal bovine serum.

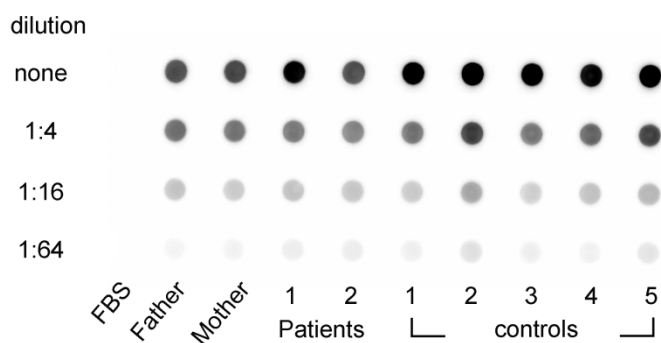


Figure 6. Comparison between ST3GAL3 and B4GALNT1 variants. HEK-293T cells were transiently co-transfected with pcDNA3-based plasmids carrying the WT or p.A13D ST3GAL3 variant, or the WT or p.R300C B4GALNT1 variant, and luciferase expression plasmids, as an internal control for normalizing transfection efficiency, and processed as in Figure 2A. (A) Transfected HEK-293T cells were used as the enzyme source for determining the kinetics of ST3GAL3 activity toward asialo- α 1-acid glycoprotein (asialo-AGP). Asialo-AGP was assumed to contain 454 nmoles of potential Gal acceptor sites per mg of protein (Weinstein et al. 1982). Results are shown as a Hanes-Woolf plot of the activity values obtained. In the case of the p.A13D variant, activity is presented as simple duplicate values because they did not allow for Hanes-Woolf plotting. Luciferase activities in the homogenates obtained from the WT and p.A13D variant were 86% identical. (B) Transfected HEK-293T cells were used as the enzyme source for determining the kinetics of B4GALNT1 toward GM3. Results are shown as in A. Luciferase activities in the homogenates obtained from the WT and B4GALNT1 variant were 92% identical. Note the different scales used for the WT and enzyme variant in both cases.

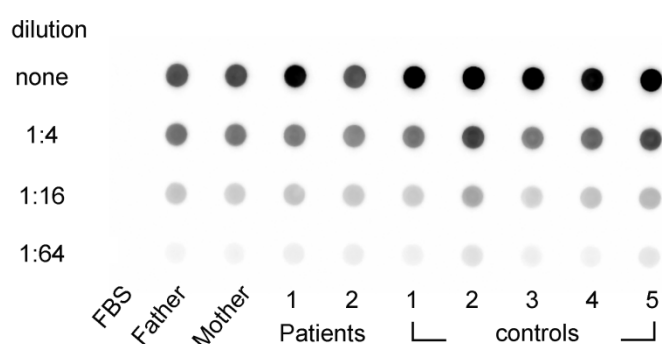


Table I. Apparent kinetic constants of ST3GAL3, B4GALNT1, and pathogenic variants.

	ST3GAL3 WT				ST3GAL3 A13D		
Acceptor ^a	Vmax ($\mu\text{mol}/\text{mg}/\text{h}$)	Km (μM)	Vmax/Km		Vmax ($\mu\text{mol}/\text{mg}/\text{h}$)	Km (μM)	Vmax/Km
LNB- <i>p</i> -NP	4.30×10^3	206	20.1		0.86×10^3	1360	0.63
Asialo-GM1	3.66×10^3	37.5	97.4		1.11×10^3	281	3.95
Lc4	2.51×10^3	5.45	460		Nd ^b	Nd	
Asialo-AGP	4.16×10^3	61.0	68.1		Nd ^b	Nd	
GM1	Nd	Nd			Nd	Nd	

	B4GALNT1 WT				B4GALNT1 R300C		
	Vmax ($\mu\text{mol}/\text{mg}/\text{h}$)	Km (μM)	Vmax/Km		Vmax ($\mu\text{mol}/\text{mg}/\text{h}$)	Km (μM)	Vmax/Km
GM3	65.6×10^3	235	279		1.86×10^3	210	8.85

Nd: not determinable

^a LNB-*p*NP, *para*-nitrophenyl-lacto-N-biose, Gal β 1,3GlcNAc β 1-O-C₆H₄NO₂; asialo-GM1, gangliotetraosylceramide; Lc4, lactotetraosylceramide; asialo-AGP, asialo-a₁ acid glycoprotein.

^bA small activity was measurable over the background that did not allow kinetic calculations (see Figure 6A and supplementary Figure S2). The Hanes-Woolf plots utilized for the calculations are presented in Figure 6 and supplementary Figure S2.